Interfacing Spins in an InGaAs Quantum Dot to a Semiconductor Waveguide Circuit Using Emitted Photons

I. J. Luxmoore,[1,*] N. A. Wasley,[1] A. J. Ramsay,[1,2] A. C. T. Thijssen,[3] R. Oulton,[3] M. Hugues,[4] S. Kasture,[5] V. G. Achanta,[5] A. M. Fox,[1] and M. S. Skolnick[1]

[1]*Department of Physics and Astronomy, University of Sheffield, Sheffield S3 7RH, United Kingdom*
[2]*Hitachi Cambridge Laboratory, Hitachi Europe Ltd, Cambridge CB3 OHE, United Kingdom*
[3]*H.H. Wills Physics Laboratory, Tyndall Avenue, Bristol BS8 1TL, United Kingdom*
[4]*Department of Electronic and Electrical Engineering, University of Sheffield, Sheffield S1 3JD, United Kingdom*
[5]*DCMP and MS, Tata Institute of Fundamental Research, Mumbai 400 005, India*

(Received 10 July 2012; published 14 January 2013)

An in-plane spin-photon interface is essential for the integration of quantum dot spins with optical circuits. The optical dipole of a quantum dot lies in the plane and the spin is optically accessed via circularly polarized selection rules. Hence, a single waveguide, which can transport only one in-plane linear polarization component, cannot communicate the spin state between two points on a chip. To overcome this issue, we introduce a spin-photon interface based on two orthogonal waveguides, where the polarization emitted by a quantum dot is mapped to a path-encoded photon. We demonstrate operation by deducing the spin using the interference of in-plane photons. A second device directly maps right and left circular polarizations to antiparallel waveguides, surprising for a nonchiral structure but consistent with an off-center dot.

DOI: 10.1103/PhysRevLett.110.037402 PACS numbers: 78.67.Hc, 03.67.Lx

The spin of a quantum dot (QD) makes a good static qubit with microsecond regime coherence times [1,2] and radiative lifetime limited optical transitions [3]. A promising approach to build a register of qubits is to use a network of spatially separated QDs with a manageable energy spectrum, connected by photons. A number of key experimental demonstrations towards this goal have been reported, including highly tunable QDs [4,5], nonclassical light sources [6–8], strong coupling [9,10], indistinguishable photons from two remote QDs [11,12], and on-chip integration with single photon detectors [13]. Conceptually, the most obvious way to think of transmitting spin information is to use the polarization state of the photon, since the spin of a recombining QD exciton and the polarization of the emitted photon are related by strict selection rules. However, this is not compatible with a planar photonic circuit, which is essential for integration [14]. The fundamental problem is that, due to strong vertical confinement, the optical dipole of a self-assembled QD lies in the xy plane, and since only the x or y linear polarization component of the left or right $[\sigma^{\pm} = (x \pm iy)/\sqrt{2}]$ circularly polarized light can propagate along a waveguide, the in-plane transfer of spin information is inhibited. Even the most basic question of how to optically detect a spin using in-plane photons has not, until now, been addressed.

In this Letter we propose and demonstrate a spin to guided-photon interface. A scanning electron microscope image of the prototype device employed is presented in Fig. 1(a). The device consists of two orthogonal freestanding waveguides with a width of ~200 nm connected to four outcouplers [15]. The waveguides are fabricated from a 140 nm thick GaAs layer containing a single layer of InGaAs QDs at its center.

Because of strict selection rules, when an exciton recombines it emits a photon with a polarization that can be mapped to the pseudospin of the exciton. In the case of a charged QD, the spin of the resident carrier can then be inferred from Pauli blocking. Here we present results for a neutral exciton transition, but the demonstration holds for all charge states of the QD. A QD located at the center of the waveguide intersection will coherently emit the $x(y)$-polarization component of a circularly polarized state into the waveguides aligned along the $y(x)$ directions, respectively. By collecting both polarization components, while retaining their relative phase, the full polarization state of the photon is mapped to a path-encoded state. On recombining the light from the waveguides, the polarization state of the photon can be reconstructed at another point in the plane, hence enabling on-chip transfer of spin information.

Finite difference time domain (FDTD) simulations [16] reveal that the spin to path conversion is sensitive to the QD position. We present experimental results from two devices. For device A, consistent with a QD located near the center of the intersection, the coherent transfer of the full polarization of the photon emitted by the QD to the path-encoded state is demonstrated. By contrast, in device B, consistent with the QD located off center, the σ^{+} and σ^{-} polarization components are mapped to different waveguides enabling direct readout of the up or down state of the QD spin. Unexpectedly, in this case inversion symmetry between propagation along forward and backward

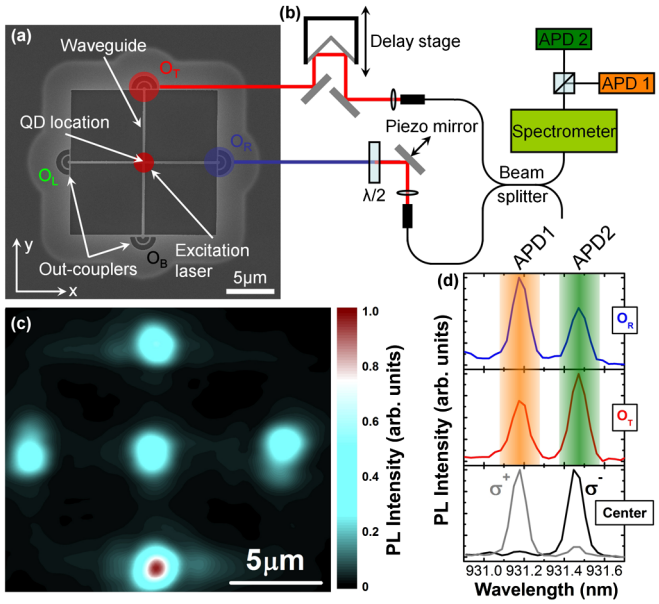

FIG. 1 (color online). Prototype spin-photon interface and experimental setup. (a) Scanning electron microscope image of the device. Two orthogonal nanowire waveguides are excited at their intersection by a cw laser, linearly polarized at 45° to the x axis. QD emission into the two waveguides is measured via outcouplers, which scatter light into the z direction. O_T, O_R, O_B, and O_L signify the top, right, bottom, and left outcouplers, respectively. (b) Schematic diagram of the optical setup used in the spectroscopy and interference experiments. (c) PL intensity map, integrated over the QD distribution, recorded from the spin-photon interface, by scanning the collection fiber with the excitation laser fixed at the intersection. (d) PL spectra recorded from a single Zeeman split QD line at the intersection and two outcouplers of device A. At the intersection the transitions of the Zeeman doublet are found to be right and left circularly polarized, as expected. From the orthogonal outcouplers, O_R and O_T, both σ^+ and σ^- transitions are observed. The orange (left) and green (right) shaded regions indicate the spectral windows, corresponding to σ^+ and σ^- emission, respectively, collected by the two APDs in the interference experiments shown in Fig. 2.

aligned waveguides is broken. This result is in good agreement with the FDTD simulations, which show that an arbitrary spin state can still be transferred via a pair of waveguides when the QD is off center, making the technique robust to QD alignment accuracy.

The demonstration of the principle proceeds by several steps. First, a laser is used to excite the QD wetting layer at the intersection. A map of the photoluminescence (PL), integrated over the QD ensemble, is presented in Fig. 1(c). Strong emission is observed from all four outcouplers and the intersection. This verifies that emission from the QDs excited at the waveguide intersection is transmitted along the waveguides and scattered vertically by the outcouplers.

The next step is to identify a device in which a single QD emits into two orthogonal waveguides. The structure is again excited at the intersection and PL spectra measured at the intersection and the outcouplers, labeled O_R and O_T in Fig. 1(a), are compared. A magnetic field, $B = 3$ T, is applied normal to the sample plane, so that the σ^+ and σ^- polarized transitions can be identified by their characteristic energies. Figure 1(d) shows the PL spectrum for the Zeeman split doublet originating from a QD located at the intersection of device A. When observed vertically from the intersection, polarization sensitive detection confirms that the two transitions are right and left circularly polarized. Both transitions can also be observed from all four outcouplers, with the spectra recorded from O_R and O_T shown in Fig. 1(d). The contrast C_α between the $\sigma^\pm$ lines observed from the outcouplers, defined as $C_\alpha = (I^+ - I^-)/(I^+ + I^-)$, where $I^+(I^-)$ is the PL intensity of the $\sigma^+(\sigma^-)$-polarized transition and $\alpha = T, R$ are $C_R = -0.19$ and $C_T = +0.19$, respectively. This is consistent with mapping horizontal and vertical linear polarizations to the orthogonal waveguides, and is close to the desired value of $C_\alpha = 0$. To verify that the QD is a single photon emitter, the second-order correlation function is measured and clear antibunching observed. Using Fourier-transform spectroscopy, the coherence times for the QDs of devices A and B are found to be ~100 and ~68 ps, respectively. This is typical of InGaAs QDs in nanophotonic structures [17,18], but shorter than values reported for QDs in the bulk [3]. The characterization of the QDs is presented in Sec. S1 of the Supplemental Material [19].

Finally, in the ideal case, a $\sigma^\pm$-polarized photon emitted by the QD will be mapped to the top and right waveguides such that $|x\rangle \pm i|y\rangle \rightarrow |T\rangle \pm i|R\rangle$. To demonstrate this we use an interference experiment as depicted in Fig. 1(b). Emission from the top and right waveguides is collected by two fibers and recombined using a fiber beam splitter. The first-order interference of the photoluminescence of the σ^+ and σ^- peaks is measured simultaneously using separate avalanche photo diodes (APDs) to demonstrate the optical coherence of photons emitted into the top and right waveguides. The interferograms of the $\sigma^\pm$ peaks are recorded simultaneously to achieve a mechanically robust measurement of their relative phase $\Delta\phi$. The relative phase between the x and y components of the $\sigma^\pm$ peaks differs by π, resulting in an expected phase shift of π between the interferograms of the $\sigma^\pm$ peaks at zero time delay.

To accurately determine time delay $t_d = 0$, the interference contrast of the entire QD ensemble is measured and plotted in Fig. 2(c). Figure 2(a) presents a plot of the intensities $I^\pm$ of the $\sigma^\pm$ peaks as the time delay is varied using a mirror mounted on a piezoelectric actuator for a coarse time delay t_d of zero. The $I^\pm$ interference signals are close to π out of phase, confirming that the spin up or down state of the QD is encoded in the relative phase between the top and bottom waveguides. In principle, if the phase delay is fixed at $\pi/2$, in-plane detection of the spin is possible, since a photon emitted by a QD in the spin up or down state would exit via opposite ports of an on-chip beam splitter.

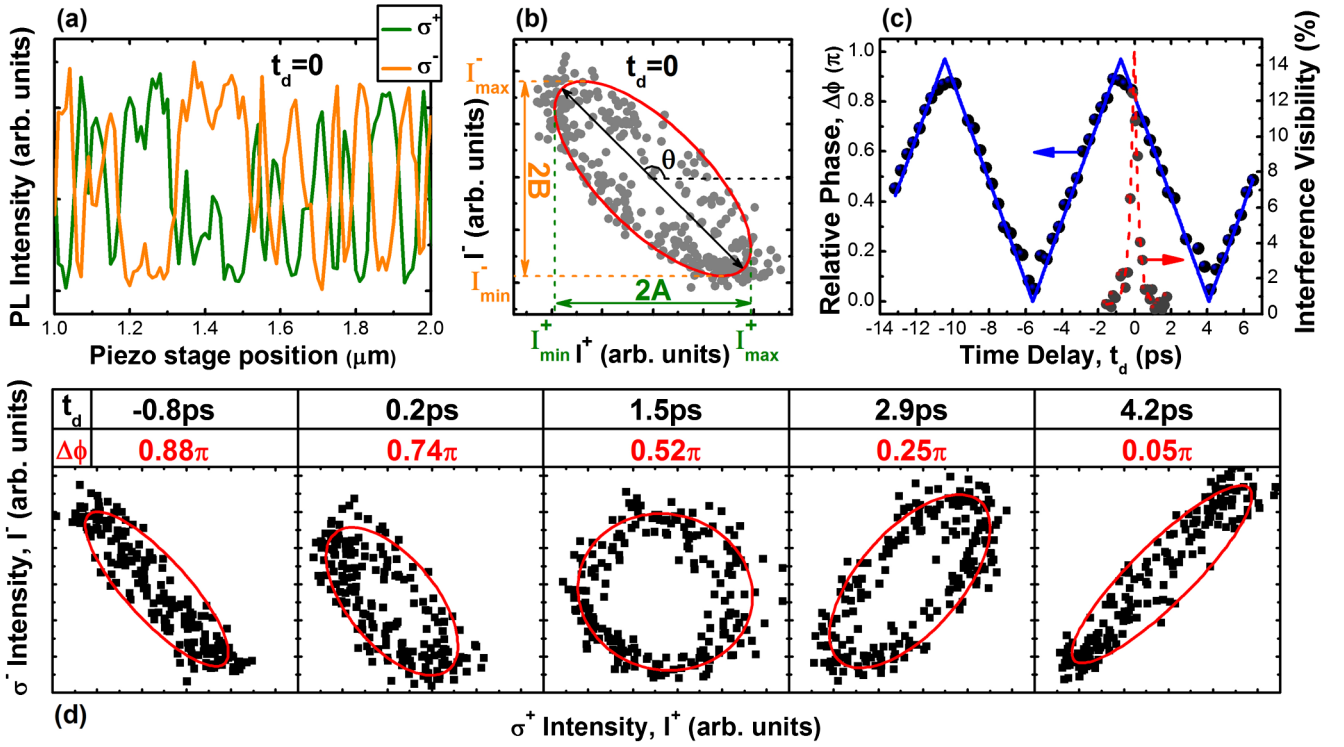

FIG. 2 (color online). Interference measurements of device A. (a) Interference fringes, for σ^+ and σ^- light detected from O_R and O_T, recorded as the piezomirror position is varied at $t_d = 0$. (b) Intensity plot of the interference data presented in (a) showing that the σ^+ and σ^- transitions are $\sim\pi$ out of phase at $t_d = 0$ and can therefore be identified using an interference measurement in an in-plane architecture. The solid red line shows a fit of an ellipse to the data, which is used to extract the relative phase between the σ^+ and σ^- transitions, from $\Delta\phi = \cos^{-1}[(A/B)\tan(\theta)]$. (c) The left-hand axis shows a plot of $\Delta\phi$ as a function of time delay. The solid blue line is a triangular waveform fit to the data. The right-hand axis plots the visibility of the white light interference of the QD distribution, which is fitted with the function, $V(t) = V_0 + V_1 e^{(t_d - t_0)/\tau}$ to determine $t_d = 0$. (d) Intensity plots of the interference fringes recorded simultaneously from the σ^+ and σ^- transitions at different delay times of the interferometer. The solid red lines show elliptical fits to the data.

To make a more accurate measurement of the relative phase $\Delta\phi$, a series of measurements of $I^{\pm}$ versus coarse time delay is made for small variations in the time delay using the piezoelectric actuated mirror. A phase plot of I^+ versus I^- results in an ellipsoid from which the relative phase and visibility can be deduced, as shown in Fig. 2(b). In Fig. 2(d), as the time delay is varied, the ellipticity of the plot oscillates between a straight line of negative gradient ($\Delta\phi = \pi$) to a straight line of positive gradient ($\Delta\phi = 0$), via a circle ($\Delta\phi = \pi/2$). The period is 10 ps, corresponding to the Zeeman splitting of 0.41 meV. The oscillation in the relative phase $\Delta\phi$ is plotted in Fig. 2(c). At zero time delay $\Delta\phi = 0.91\pi$ is deduced, close to the expected value of π. The above experiments demonstrate that for device A the polarization of the photon emitted by the QD, including the relative phase between polarization components, and hence the full spin state of the QD, is coherently mapped to a path-encoded state by the orthogonal waveguides.

Device B demonstrates markedly different behavior, with in-plane spin readout without the need for an interferometer. Figures 3(a) and 3(b) show PL spectra recorded for the Zeeman split doublet from the four outcouplers of device B with $B = 4$ T. When measuring from the outcouplers, the $\sigma^+(\sigma^-)$ polarized light is only observed from O_R and O_B (O_L and O_T). The contrasts extracted from Fig. 3(a) are $C_R = 0.92$ and $C_L = -0.93$, which corresponds to the direct readout of the spin state of the QD in an in-plane geometry.

To understand the different spin to path conversion properties of devices A and B, we use FDTD simulations to investigate the effect of QD position [19]. A circularly polarized dipole source is located in the intersection at a distance s from the center along the diagonal, as illustrated in Fig. 3(h), and the power transmitted into the four waveguides calculated. Figure 3(c) plots the calculated contrast in the waveguides as a function of s, which is strongly dependent on source position. Close to the center, light is coupled equally into all four waveguides, as observed for device A. If, however, the QD is located at $s = 90$ nm, the $\sigma^+(\sigma^-)$ polarized light is directed along the bottom and right (top and left) waveguides, reproducing the experimentally observed behavior of device B. From the simulations, we infer that for device A, $s < \sim 50$ nm, and for device B, $s \approx 90$ nm. The operation of the two devices is

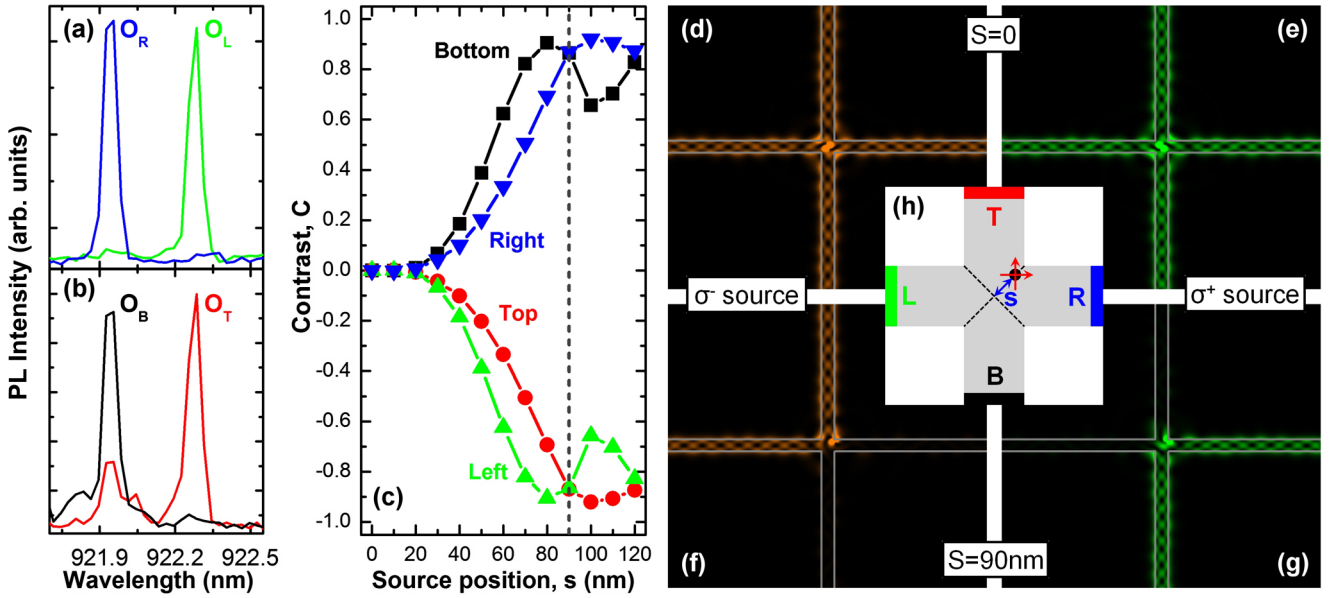

FIG. 3 (color online). Photoluminescence measurements for device B and a numerical investigation into the effects of QD position on device operation. (a) PL spectra recorded from outcouplers O_R and O_L showing pronounced asymmetry between the two antiparallel directions. (b) PL spectra recorded from O_B and O_T, again showing the pronounced asymmetry of (a). (c) FDTD simulations showing the contrast of $\sigma^{\pm}$ polarized light in each waveguide for a source located at a distance s along the diagonal from the center of the intersection. The dashed gray line indicates the location of the source for the simulations shown in (f) and (g), which reproduces well the emission properties of device B. (d)–(g) Electric field intensity $|E|^2$ at the center of the waveguides for different source locations and polarizations 0.65 ps after the cw source begins to emit. (d) σ^- polarized source located at center. (e) σ^+ polarized source located at center. (f) σ^- polarized source located off center at $s = 90$ nm. (g) σ^+ polarized source located off-centre at $s = 90$ nm. (h) Diagram illustrating the position of the source within the waveguide intersection as used in the simulations shown in (c). The dashed lines indicate the reflection planes of the diagonal and antidiagonal virtual beam splitters.

illustrated by the electric-field distribution for light emitted by $\sigma^{\pm}$ polarized dipoles as presented in Figs. 3(d) and 3(e) and Figs. 3(f) and 3(g) for $s = 0$ and $s = 90$ nm, respectively. Further calculations presented in Sec. S3 of the Supplemental Material [19] show that, despite the different spin to guided-photon maps resulting from QD location, it is possible to deduce any arbitrary spin state via a measurement of the intensity and phase at two output ports. This implies that following characterization of the device, spin to guided-photon operation can be achieved for a range of QD positions.

The different polarization to which-path conversion properties can be understood as follows. The intersection may be considered as an input or output device whose function can be simulated as a superposition of 4 beam splitters oriented every 45°. From experiments and theory [20] it is known that the backreflection is weak, and therefore the beam splitters along the x and y axes can be neglected. To conserve energy as the QD position is moved, we also deduce that the remaining two beam splitters must be 50:50.

For an x-polarized dipole, light is emitted primarily into wave vectors ky which can be treated as inputs from the top and bottom waveguides with a relative phase of π since the source is a dipole. The amplitudes of the output ports are then calculated as a superposition of all four combinations of input ports and beam-splitter orientation, as depicted in Fig. S4 of the Supplemental Material [19]. The amplitudes for the y-polarized dipole can also be calculated in this way. The amplitudes for any arbitrary polarization are then calculated as a superposition of the x and y dipoles. The results of this calculation are presented in Fig. S4 of the Supplemental Material [19].

If the QD is positioned at the center, the reflections into the right and left waveguides destructively interfere and the x dipole only emits into the top or bottom waveguides, as observed for device A.

If the QD is displaced along the diagonal, the reflection symmetry about the antidiagonal axis is broken and the input states of the antidiagonal beam splitter acquire a position dependent phase factor $e^{\pm iks/\sqrt{2}}$ for the top and bottom inputs, respectively. For σ^+-polarized dipole, at a position $ks/\sqrt{2} = \pi/2$, a destructive interference occurs canceling emission into the top and left waveguides, as observed for device B. For a wavelength of 920 nm, this occurs at $s = 93$ nm, close to the value deduced using FDTD, confirming this interpretation.

In summary, we have presented a scheme for interfacing an optically addressed spin qubit to a path-encoded photon using a crossed waveguide device. We have demonstrated the operation of this device in two regimes dependent on the location of the QD and have shown that it can be used

for in-plane transfer and readout of spin information. Future directions include the use of nanocavities to enhance the light-matter interactions [21] and on-chip readout using integrated single photon detectors [13]. Further work to investigate the use of path-encoded photons, which are better suited to a planar photonic circuit [14] than polarization encoded photons, to manipulate [22,23] and ultimately entangle [24] remote on-chip QD spins is also needed.

This work was funded by EPSRC Grants No. EP/G001642, No. EP/J007544, and No. EP/G004366/1, and as part of project SPANGL4Q, under FET-Open Grant No. FP7-284743. The FDTD calculations used the computational facilities of the Advanced Computing Research Centre (Bristol). We thank D. N. Krizhanovskii, L. R. Wilson, P. Kok, and D. M. Whittaker for helpful discussions and comments on the manuscript.

*Present address: College of Engineering, Mathematics and Physical Sciences, University of Exeter, Exeter EX4 4QL, United Kingdom.
i.j.luxmoore@exeter.ac.uk

[1] A. Greilich, D. R. Yakovlev, A. Shabaev, Al. L. Efros, I. A. Yugova, R. Oulton, V. Stavarache, D. Reuter, A. Wieck, and M. Bayer, Science **313**, 341 (2006).
[2] D. Brunner, B. D. Gerardot, P. A. Dalgarno, G. Wust, K. Karrai, N. G. Stoltz, P. M. Petroff, and R. J. Warburton, Science **325**, 70 (2009).
[3] P. Borri, W. Langbein, S. Schneider, U. Woggon, R. Sellin, D. Ouyang, and D. Bimberg, Phys. Rev. Lett. **87**, 157401 (2001).
[4] A. J. Bennett, R. B. Patel, J. Skiba-Szymanska, C. A. Nicoll, I. Farrer, D. A. Ritchie, and A. J. Shields, Appl. Phys. Lett. **97**, 031104 (2010).
[5] A. Laucht, F. Hofbauer, N. Hauke, J. Angele, S. Stobbe, M. Kaniber, G. Böhm, P. Lodahl, M.-C. Amann, and J. J. Finley, New J. Phys. **11**, 023034 (2009).
[6] Z. Yuan, B. E. Kardynal, R. M. Stevenson, A. J. Shields, C. J. Lobo, K. Cooper, N. S. Beattie, D. A. Ritchie, and M. Pepper, Science **295**, 102 (2002).
[7] C. L. Salter, R. M. Stevenson, I. Farrer, C. A. Nicoll, D. A. Ritchie, and A. J. Shields, Nature (London) **465**, 594 (2010).
[8] A. Dousse, J. Suffczyński, A. Beveratos, O. Krebs, A. Lemaître, I. Sagnes, J. Bloch, P. Voisin, and P. Senellart, Nature (London) **466**, 217 (2010).
[9] J. P. Reithmaier, G. Sęk, A. Löffler, C. Hofmann, S. Kuhn, S. Reitzenstein, L. V. Keldysh, V. D. Kulakovskii, T. L. Reinecke, and A. Forchel, Nature (London) **432**, 197 (2004).
[10] T. Yoshie, A. Scherer, J. Hendrickson, G. Khitrova, H. M. Gibbs, G. Rupper, C. Ell, O. B. Shchekin, and D. G. Deppe, Nature (London) **432**, 200 (2004).
[11] R. B. Patel, A. J. Bennett, I. Farrer, C. A. Nicoll, D. A. Ritchie, and A. J. Shields, Nat. Photonics **4**, 632 (2010).
[12] E. Flagg, A. Muller, S. V. Polyakov, A. Ling, A. Migdall, and G. S. Solomon, Phys. Rev. Lett. **104**, 137401 (2010).
[13] J. P. Sprengers *et al.*, Appl. Phys. Lett. **99**, 181110 (2011).
[14] J. L. O' Brien, A. Furusawa, and J. Vuckovic, Nat. Photonics **3**, 687 (2009).
[15] A. Faraon, I. Fushman, D. Englund, N. Stoltz, P. Petroff, and J. Vuckovic, Opt. Express **16**, 12 154 (2008).
[16] A. F. Oskooi, D. Roundy, M. Ibanescu, P. Bermel, J. D. Joannopoulos, and S. G. Johnson, Comput. Phys. Commun. **181**, 687 (2010).
[17] C. Santori, D. Fattal, J. Vučković, G. S. Solomon, and Y. Yamamoto, Nature (London) **419**, 594 (2002).
[18] S. Laurent, S. Varoutsis, L. L. Gratiet, A. Lemaıtre, I. Sagnes, F. Raineri, A. Levenson, I. Robert-Philip, and I. Abram, Appl. Phys. Lett. **87**, 163107 (2005).
[19] See Supplemental Material at http://link.aps.org/supplemental/10.1103/PhysRevLett.110.037402 for supporting measurements and FDTD simulations.
[20] S. G. Johnson, C. Manolatou, S. Fan, P. R. Villeneuve, J. D. Joannopoulos, and H. A. Haus, Opt. Lett. **23**, 1855 (1998).
[21] K. Rivoire, S. Buckley, and J. Vuckovic, Opt. Express **19**, 22 198 (2011).
[22] D. Press, T. D. Ladd, B. Zhang, and Y. Yamamoto, Nature (London) **456**, 218 (2008).
[23] T. M. Godden, J. Quilter, A. Ramsay, Y. Wu, P. Brereton, S. Boyle, I. Luxmoore, J. Puebla-Nunez, A. Fox, and M. Skolnick, Phys. Rev. Lett. **108**, 017402 (2012).
[24] S. D. Barrett and P. Kok, Phys. Rev. A **71**, 060310 (2005).